

## ANALYSIS OF EFFECT OF TIRE MATERIAL ON THE PREDICTION OPTIMUM TREAD SECTIONS

S K Deb Nath, S Reaz Ahmed and M Wahajuddin

Department of Mechanical Engineering  
Bangladesh University of Engineering and Technology, Dhaka 1000, Bangladesh

### ABSTRACT

An ideal mathematical model for the practical stress problems, namely, the displacement potential function formulation has been used in conjunction with the finite-difference method of solution for the present analysis. For the analysis, first, the contact surface of the tire tread is assumed to be free from frictional force. The results of this frictionless analysis however give the basis for realizing the fact that the continuous lateral slipping action of the tread contact surface on the road plays the most important role in shortening the life of tires as far as the wear is concerned. Based on the analysis, a method is proposed to determine the optimum tread shapes of several tire material for avoiding lateral slippage between tires and roads. Finally, the maximum calculated coefficient of friction obtained from the maximum shearing stress, of the tire tread of three different tire material such as natural rubber, truck tire rubber and retreaded rubber are analyzed in the perspective of tread aspect ratio, where the dimensions of the tread section are varied in both the normal and lateral directions. From the comparison of the calculated coefficient of friction with the friction coefficient available from the road, an optimum value of the aspect ratio for the tire tread of three different tire material is determined, which ensures no wear of tire tread due to the lateral slipping of the contact surface on the road.

**Keywords:** Finite difference method, Calculated maximum coefficient of friction, Displacement potential function.

### 1. INTRODUCTION

Rubber tires are considered as one of the indispensable components of almost all categories of automotive vehicles. Technical reporting on the analysis and design of rubber tires and treads for various automotive vehicles is quite extensive [1-11] and [13-14]. Luper H. *et al.* [1] stated TROWS (Tire and road wear and slip assessment). One of the TROWS objectives is to provide a tool table to numerically predict tire global wear as well as to qualitatively determine the wear distribution. Han Y. H. *et al.* [2] presented a new three-dimensional finite element local model to calculate the energy release rate at the belt region. Colby D. *et al.* [3] analyzed on pattern recognition for classification and matching of car tires. Kao B.G. *et al.* [4] studied the bushing analogy Tire (BAT) model for tire dynamics modeling in vertical and lateral directions cover the tire modes in those directions up to about 100 HZ. Hall W. and Mottram J. T [5] developed tire modeling methodology with the explicit finite element code LS-DYNA. This model was applied for static and dynamic conditions separately. Olatunbosun O. A. and Bolarinwa O. [6] presented a three dimensional finite element tire model developed using ABAQUS, a commercial finite element code for use in the

development of new tire designs and simulation of vehicle. Chen B. [7] analyzed material characterization of tire cords and the effects of cord thermal mechanical properties on tire by using finite element method. A number of authors have focused, especially, on the analysis of stresses and deformed shapes of reinforced tires by finite element method [8-11]. Some of the papers [10-11] considered the static tire contact problem for obtaining the deformation patterns and stress-state in the tire cross-section without paying attention to the bending effect of the reinforced cords. Taking the bending effect into consideration and laying emphasis on it during shear deformation of elements, Huh and Kwak [9] developed the expressions of effective material properties of rubber composites, and applied to the inflation and contact problem of reinforced tire. Wang *et al.* [10] reported an experimental stress-strain analysis by means of the Moire method in the area of the shoulder region of a retreaded tire section. They also presented a comparison of the experimental results with those obtained by finite element method. The specimen for the experiment was a cross-sectional slice of a retreaded truck tire. Some of the papers [13-14] presented mechanical properties of tire rubber and optimization of the size of tire treads.

The present paper describes a new numerical approach to predict the optimum shapes of tire treads considering three different tire materials by using the displacement potential formulation.

## 2. DISPLACEMENT POTENTIAL FORMULATION FOR THE PROBLEM

In order to formulate the two dimensional elastic problems in terms of displacement potential function,  $\psi$ , both the equilibrium equations and the boundary conditions are required to be expressed in terms of the displacement components  $u_x$  and  $u_y$ . In absence of body forces, the equilibrium equations for two-dimensional elastic problems in terms of displacement components are,

$$\frac{\partial^2 u_x}{\partial x^2} + \left(\frac{1-\mu}{2}\right) \frac{\partial^2 u_x}{\partial y^2} + \left(\frac{1+\mu}{2}\right) \frac{\partial^2 u_y}{\partial x \partial y} = 0 \quad (1)$$

$$\frac{\partial^2 u_y}{\partial y^2} + \left(\frac{1-\mu}{2}\right) \frac{\partial^2 u_y}{\partial x^2} + \left(\frac{1+\mu}{2}\right) \frac{\partial^2 u_x}{\partial x \partial y} = 0 \quad (2)$$

Where  $u_x$  and  $u_y$  are the displacement components of a point in the  $x$  and  $y$  directions, respectively. These two homogeneous elliptical partial differential equations with the appropriate boundary conditions should be sufficient for the evaluation of the two functions  $u_x$  and  $u_y$ , and the knowledge of these functions over the region concerned will uniquely determine the stress components.

Although the above two differential equations are sufficient to solve mixed boundary-value elastic problems, but in reality, it is difficult to solve for two functions simultaneously. So, to overcome this difficulty, equations (1) and (2) are converted into a single equation, using a potential function. If a function is defined in terms of the displacement components  $u_x$  and  $u_y$ , then the determination of that function uniquely determines the stress functions sought for. The present potential function approach involves investigation of the existence of a function defined in terms of the displacement components. In this approach, as in the case of Airy's stress function, the problem is reduced to the determination of a single variable. The potential function  $\psi(x,y)$  is defined in terms of displacement components as,

$$u_x = \frac{\partial^2 \psi}{\partial x \partial y} \quad (3)$$

$$u_y = -\left[\left(\frac{1-\mu}{1+\mu}\right) \frac{\partial^2 \psi}{\partial x^2} + \left(\frac{2}{1+\mu}\right) \frac{\partial^2 \psi}{\partial x^2}\right] \quad (4)$$

With this definition of  $\psi(x, y)$ , the first of the two equations (1) and (2) is automatically satisfied. Therefore,  $\psi$  has only to satisfy the compatibility equation. Expressing this equation in terms of  $\psi$ , the condition that  $\psi$  has to satisfy becomes,

$$\frac{\partial^4 \psi}{\partial x^4} + 2 \frac{\partial^4 \psi}{\partial x^2 \partial y^2} + \frac{\partial^4 \psi}{\partial y^4} = 0 \quad (5)$$

In order to solve the problem in terms of the potential The boundary conditions should also be expressed in terms of  $\psi$ . The boundary conditions are prescribed as known restraints and loadings, that is, known values of components of stresses and displacements on the boundary. The relations between the known functions on the boundary and the function  $\psi(x,y)$  are

$$u_x = \frac{\partial^2 \psi}{\partial x \partial y} \quad (6)$$

$$u_y = -\left[\left(\frac{1-\mu}{1+\mu}\right) \frac{\partial^2 \psi}{\partial x^2} + \left(\frac{2}{1+\mu}\right) \frac{\partial^2 \psi}{\partial x^2}\right] \quad (7)$$

$$\begin{aligned} \sigma_{xx} &= \left(\frac{E}{1-\mu^2}\right) \left(\frac{\partial u}{\partial x} + \mu \frac{\partial v}{\partial y}\right) \\ &= \frac{E}{(1+\mu)^2} \left[\frac{\partial^3 \psi}{\partial x^2 \partial y} - \mu \frac{\partial^3 \psi}{\partial y^3}\right] \end{aligned} \quad (8)$$

$$\begin{aligned} \sigma_{yy} &= \left(\frac{E}{1-\mu^2}\right) \left(\frac{\partial u_y}{\partial y} + \mu \frac{\partial u_x}{\partial x}\right) \\ &= \frac{E}{(1+\mu)^2} \left[\frac{\partial^3 \psi}{\partial x^2 \partial y} + (\mu+2) \frac{\partial^3 \psi}{\partial x^2 \partial y}\right] \end{aligned} \quad (9)$$

$$\begin{aligned} \sigma_{xy} &= \frac{E}{2(1+\mu)} \left(\frac{\partial u_x}{\partial y} + \mu \frac{\partial u_y}{\partial x}\right) \\ &= \frac{E}{(1+\mu)^2} \left[\mu \frac{\partial^3 \psi}{\partial x \partial y^2} - \frac{\partial^3 \psi}{\partial x^3}\right] \end{aligned} \quad (10)$$

## 3. SOLUTION PROCEDURE

### 3.1 Method of Solution

The mixed boundary value problem is unquestionably beyond the scope of pure analytical methods of solutions. Thus numerical solution for this class of problems is the only plausible approach. Here, finite difference technique is used to discretize the bi-harmonic partial differential equation and also the differential equations associated with the boundary conditions. The discrete values of the displacement potential function  $\psi(x,y)$ , at the mesh points of the domain Fig.1(b) concerned, is solved from the system of linear algebraic equations resulting from the discretization of the bi-harmonic equation and the associated boundary conditions.

### 3.2 Discretization of the Domain

According to the usual practice, the region in which a dependent function is to be evaluated is divided into a desirable number of mesh points and the values of the function are sought only at these mesh points. The present program is to solve a function within a stepped rectangular region, which is divided into meshes with lines parallel to rectangular co-ordinate axes. As a result,

the boundary may not always pass through the mesh points of rectangular networks. But the physical problems are associated with the known boundary conditions at the boundary points of arbitrary shaped bodies. It requires a further treatment to relate the values on the boundary with the field grid points. The governing bi-harmonic equation, which is used to evaluate the function  $\psi$  at the internal mesh points, is expressed in its corresponding difference equation using central difference operators. When all the derivatives present in the bi-harmonic equation are replaced by their respective central difference formulae, the complete finite difference expression for biharmonic equation becomes

$$\begin{aligned}
& R^4 \{ \psi(i-2, j) \} - 4R^2 (1 + R^2) \\
& \{ \psi(i-1, j) + \psi(i+1, j) \} \\
& - 4(1 + R^2) \{ \psi(i, j+1) + \psi(i, j-1) \} \\
& + (6R^4 + 8R^2 + 6) \psi(i, j) \\
& + 2R^2 \left\{ \begin{aligned} & \psi(i-1, j-1) + \psi(i-1, j+1) \\ & + \psi(i+1, j-1) + \psi(i+1, j+1) \end{aligned} \right\} \\
& + \psi(i, j-2) + \psi(i, j+2) = 0
\end{aligned} \tag{11}$$

### 3.3 Management of Boundary Conditions

Normally, the boundary conditions are specified either in terms of loadings or of restraints or of some combination of two. Each mesh point on the physical boundary of the domain always entertains two of the four possible boundary conditions at a time namely, (1) normal stress and shear stress; (2) normal stress and tangential displacement; (3) shear stress and normal displacement; (4) normal displacement and tangential displacement. The computer program is organized here in such a fashion that, out of these two conditions, one is used for evaluation of  $\psi$  at the concerned boundary point and the other one for the corresponding point on the exterior false boundary. Thus, when the boundary conditions are expressed by their appropriate difference equations, every mesh point of the domain will have a single linear algebraic equation tagged to it for its evaluation. The boundary of the tread section is divided into four segments, namely, (a) the top-left, (b) the bottom left, (c) the bottom right, and (d) the top right. Four different sets of boundary expressions are used for the four segments.

## 4. RESULTS AND DISCUSSION

For the solution of the problem, three different tire materials are taken such as Natural rubber, Retreaded rubber and Truck tire rubbers which exist three different mechanical properties. These mechanical properties are found by experimentally which require for the solution of the problem. At first the contact surface of the boundary is assumed to be smooth and secondly it is assumed that the contact surface of the tread with the road exist no slipping.

Table 1: Mechanical properties of different Tire material

Tire material	Natural rubber	Truck Tire Tread rubber	Retreaded rubber
Modulus of Elasticity (kPa)	4854	7031	8855
Poisson's ratio	0.50	0.43	0.40

Table 2: Boundary conditions of different boundary segment of the tread section considering no frictional effect of the contact surface with the road

Boundary segment	Given boundary conditions	Physical boundary conditions	False boundary conditions
AB	$u_n, u_t$	$u_t$	$u_n$
BC	$\sigma_n, \sigma_t$	$\sigma_n$	$\sigma_t$
CD	$\sigma_n, \sigma_t$	$\sigma_n$	$\sigma_t$
DE	$u_n, \sigma_t$	$u_n$	$\sigma_t$
EF	$u_n, u_t$	$u_t$	$u_n$
FG	$u_n, \sigma_t$	$u_n$	$\sigma_t$
GH	$\sigma_n, \sigma_t$	$\sigma_n$	$\sigma_t$
AH	$\sigma_n, \sigma_t$	$\sigma_n$	$\sigma_t$

Table 3: Boundary conditions of different boundary segment of the tread section considering no slipping action of the contact surface with the road

Boundary segment	Given boundary conditions	Physical boundary conditions	False boundary conditions
AB	$u_n, \sigma_t$	$\sigma_t$	$u_n$
BC	$\sigma_n, \sigma_t$	$\sigma_n$	$\sigma_t$
CD	$\sigma_n, \sigma_t$	$\sigma_n$	$\sigma_t$
DE	$u_n, \sigma_t$	$u_n$	$\sigma_t$
EF	$u_n, u_t$	$u_t$	$u_n$
FG	$u_n, \sigma_t$	$u_n$	$\sigma_t$
GH	$\sigma_n, \sigma_t$	$\sigma_n$	$\sigma_t$
AH	$\sigma_n, \sigma_t$	$\sigma_n$	$\sigma_t$

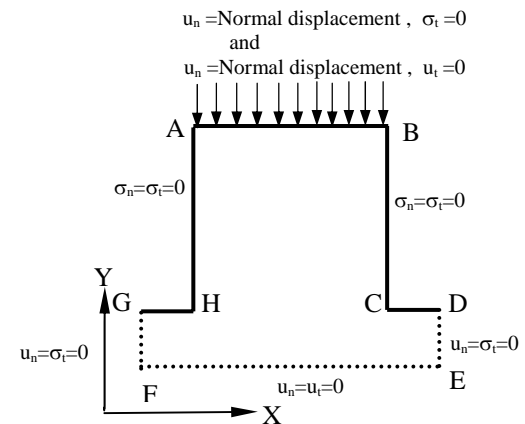


Fig 1(a). Boundary conditions and values of the Tire Tread section for the frictionless contact surface

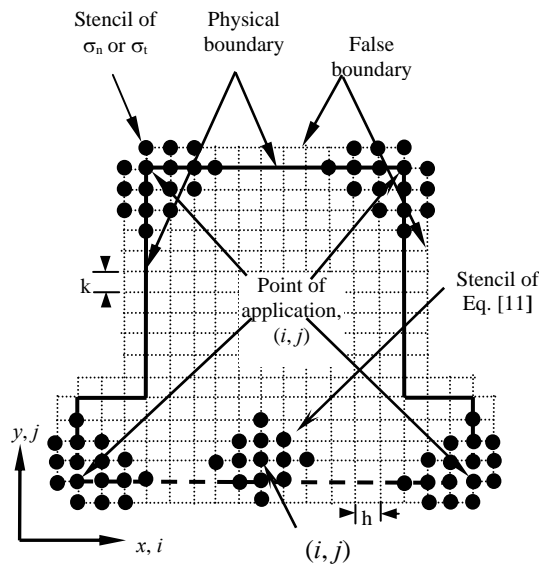


Fig 1(b). Application of the stencils of stress boundary conditions at different corners of the tread section

#### 4.1 Solution of Tire Tread Contact Problem of Different Tire Material

##### (a) Considering no frictional effect of the contact surface of the tire tread with the road

In this section, the tire-tread contact problem is obtained without considering the influence of friction on the tread surface in contact. For the analysis, three different tire materials are considered such as Natural rubber, Truck tire rubber and Retreaded rubber. That is, the tread contact surface will be allowed to deform both normally and laterally, without experiencing any frictional resistance from the road. It is important to note that the corresponding deformed shapes of the tire tread of three different tire material gives the basis for the determination of optimum sizes of tire treads for the tire tread of three different tire material. The geometry and loadings used for the solution of the frictionless tire-tread stress problem is shown in Fig.1(a). The mechanical properties of three different tire materials are shown in Table 1. The relevant boundary conditions, which have been satisfied by different segments of the tread section considering no frictional effect as well as no slipping effect are listed in Tables 2 and 3 respectively.

The uniform normal displacement considered in the present analysis corresponds to the internal inflation pressure of the tire, for example 690 kPa. The deformed shapes of the tire tread of three different tire material are shown in Fig.2(a). Figure 2(b) describes the distribution of the lateral displacement along the contact boundary of the tread ( $a/b=2.1$ ) under frictionless slipping. At the middle portion of the contact surface of each tread section, the lateral displacement is zero.

At first half portion of the contact surface, the lateral displacement is negative and at the second half portion of the contact surface, the lateral displacement is positive. The lateral displacement of the tire tread of natural rubber is very high and the lateral displacement is lower for the tire tread of retreaded rubber and the lateral displacement of the contact surface of the truck tire tread

remains between them.

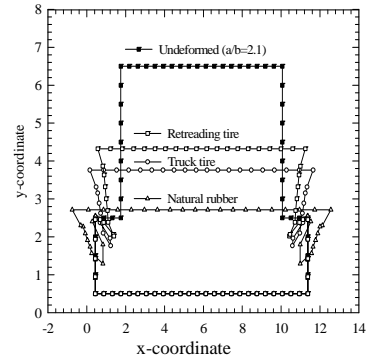


Fig 2(a). Deformed shapes of tire treads of different materials under the contact pressure of 690 kPa considering frictionless slipping

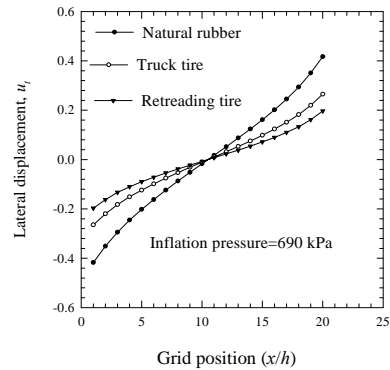


Fig 2(b). Distribution of the lateral displacement along the contact boundary of the treads ( $a/b=2.1$ ) under frictionless slipping

##### (b) No-slip condition of the contact surface of the tire tread with the road

The no slip condition of the contact boundary is actually referred to the case where the lateral displacement of the boundary, caused by the application of the uniform normal compression from the road surface, is restrained. Figure 3(a) illustrates the effect of tire material on the deformed shape of the tread section under no-slip condition of the contact boundary. The normal

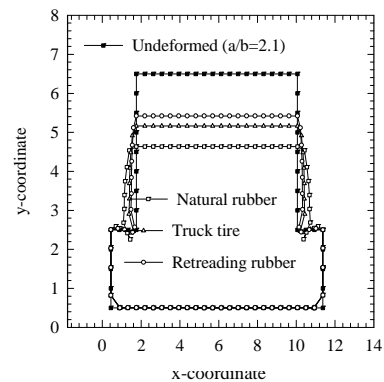


Fig 3(a). Effect of tire material on the deformed shape of the tread section under no-slip condition of the contact boundary (displacement magnified 3 times)

displacement of the tire tread of natural rubber is very high, is very low for the tire tread of retreaded rubber and the normal displacement of the contact surface of the tread of truck tire rubber remains between them. There is also significant material effect on the normal displacement of the skid surface (AH; as shown in Fig.1(a)) of the tread section.

#### 4.2 Determination of Optimum Tread Shapes Considering Different Tire Material

An analysis of the maximum stress presented in Fig.3(b) reveals that the maximum shear stress increases almost linearly with the decrease of aspect ratio and then remains nearly constant for the lower aspect ratios when the contact length is fixed. For a particular size of tire tread, the maximum shear stress is maximum for the tire tread of natural rubber and lower for the tire tread of retreaded rubber and the maximum shear stress of truck tire tread remains between them.

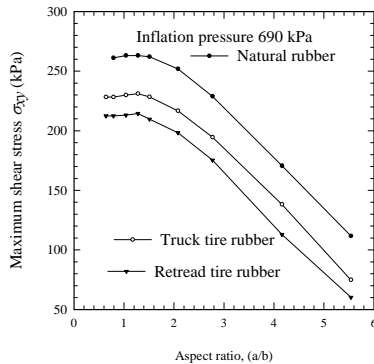


Fig 3(b). Maximum shear stress (frictional stress) as a function of tread sizes for different tire material (a is kept constant)

Figure 3(c) describes the calculated maximum coefficient of friction of tread sizes for different tire materials when the contact length is fixed. Here, according to the Coulomb's law of friction, the calculated coefficient of friction is obtained by dividing the shearing stress developed on the contact surface by the contact pressure. Table 4 lists some of the coefficients of friction for different kinds of tire with the road surface at different speed as well as for different conditions. A value of coefficient between the road and the contact surface of smooth truck tire, for example, 0.28, divides the treads in Figs.3(c) and 3(d) into two categories. In Fig.3(a), the left and right portions of the vertical line correspond to the tread sections experiencing partial slip and no-slip conditions respectively. The sizes of a tire tread for three different tire material remains in the no-slip region, there occurs no slip on the contact surface. For no slipping condition, there is larger aspect ratio for the tire tread of Natural rubber, lower aspect ratio of retreaded rubber and the aspect ratio for the tire tread of truck tire rubber remains between them. Figure 3(d) describes the calculated maximum coefficient of friction as a function of tread sizes for three different tire materials when the skid depth is kept fixed. The size of a tire tread for three different tire material remain in the no-slip zone, there occurs no slip. For no slipping

condition, there is also small aspect ratio for the tire tread of natural rubber and higher aspect ratio for the tire tread of retreaded rubber and the aspect ratio for the tire tread of truck tire rubber remains between them.

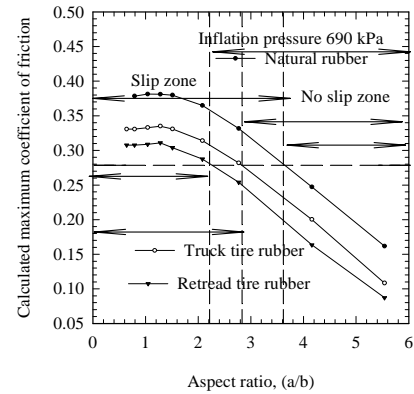


Fig 3(c). Calculated maximum coefficient of friction as a function of tread sizes for different tire materials (a is kept constant)

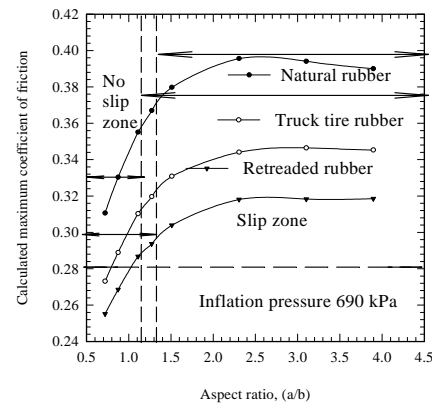


Fig 3(d). Maximum calculated coefficient of friction as a function of tread size for different tire materials when the skid depth is fixed

Table 4: Coefficient of friction by the tests of The Goodrich Company on wet pavement with tires of different treads [12]

Condition	Static (before slipping)		Sliding (before slipping)	
	5	30	5	30
Speed (mile/ h)				
Smooth tire	0.49	0.28	0.43	0.26
Circumferential groove	0.58	0.42	0.52	0.36
Angular grooves at 60°	0.75	0.55	0.70	0.39
Angular grooves at 45°	0.77	0.55	0.68	0.44

## 5. CONCLUSIONS

No serious attempt has been reported so far in the literature that can provide a useful analysis of the tread contact problem for suggesting an effective guideline to determine the optimum shapes of tire treads considering several tire materials. In this analysis it is obviously observed that slippery action of the contact surface of the tire tread of natural rubber is very high and very low for the tire tread of retreaded rubber and the slippery action of the contact surface of the tire tread of truck tire remains in between them. From the analysis, it is clear that, the sizes of the tire tread of three different tire materials which remain in the no-slip zone, the contact surface of the tire tread does not slip. For the cause of slippery action, no wear is concerned in such sizes of tire tread of three different tire materials. For avoiding slippery action, the skid depth and contact length of the tire tread of natural rubber is very larger than that of other two different tire material and the skid depth and contact length of the tire tread of retreaded rubber is very lower than that of other two different tire material.

## 6. REFERENCES

- Lupker H. Cheli F., Braghin F., Gelosa E., and Keckman A., 2004 “ Numerical prediction of car tire Wear”, *Tire science and Technology*, 32: 164-186.
- Han Y. H., Becker E. B., Fahrenthold E. P., and Kim D. M., 2004, “Fatigue life prediction for cord-rubber composite tires using a Global-Local finite element method”, *Tire science and Technology*, 32: 23-40.
- Colbry D., Cherba D., and Luchini J., “Pattern recognition for classification and matching of car tires”, *Tire science and Technology*, 33: 2-17.
- Kao B. G. and Warholic T., 2005, “Tire lateral force modeling and bushing analogy tire model”, *Tire science and Technology*, 33: 18-37.
- Hall W., Mottram J.T, and Jones R. P., 2004, “ Tire modeling methodology with the explicit finite element code LS-DYNA”, *Tire science and Technology*, 32: 236-261.
- Olatunbosum O.A. and Bolarinwa O., 2004, “ FE simulation of effect of tire design parameters on lateral forces and moments “,*Tire science and Technology*, 32: 146-163.
- Chen B., 2004 “ Material characterization of tire cords and the effects of cord thermal-mechanical properties of tires”, *Tire science and Technology*, 32: 2-22.
- Tabaddor, F. and Stafford, J. R., 1985, “Some aspects of rubber composite finite element analysis”, 1985, *Computers & Structures*, 21: 327-339.
- Huh, H. and Kwak, Y. K., 1990, “Finite element stress analysis of the reinforced tire contact problem”, *Computers & Structures*, 36: 871-881.
- Wang, T. M., Daniel, I. M., and Huangn, K., 1996, “StressAnalysis of Tire sections”, *Tire Science and Technology*, 24: 349-366.
- Rothert, H. and Gall, R., 1986, “On the three-dimensional computation of steel-belted tires, *Tire Science and Technology*, 14: 116-124
- Marks’, *Mechanical Engineering Series*, Marks’ standard Handbook for Mechanical Engineers, (Edited by Marks’), New York .
- S. K. Deb Nath, S. Reaz Ahmed and Md. Wahhaj Uddin, “Experimental determination of mechanical properties of tire rubbers”, *3<sup>rd</sup> International conference of mechanical Engineering and 8<sup>th</sup> annual paper meet on E-manufacturing*, The institution of Engineers, Bangladesh, Dhaka, 2003, 05, 32-38.
- S. Reaz. Ahmed, S. K. Deb Nath, M. Wahhaj Uddin, “Optimum shapes of tire-treads for avoiding lateral slippage between tires and roads”, *International Journal for Numerical methods in Engineering*, 2005, 64, 729-750..

## 7. NOMENCLATURE

Symbol	Meaning	Unit
$\Psi(x,y)$	Displacement potential function	-
$E$	Modulus of Elasticity	MPa
$\sigma_n$	Normal stress	kPa
$\sigma_t$	Lateral stress	kPa
$\sigma_{xy}$	Shear stress	kPa
$u_x, u_y$	Displacement at x and y direction	m
$u_n, u_t$	Normal and Lateral displacement	m
$a$	Contact length	m
$b$	Skid depth	m

Corresponding email address:  
sankar\_20005@yahoo.com